



HAL
open science

Maternal Rat Metabolomics: Amniotic Fluid and Placental Metabolic Profiling Workflows

Alexandra Bourdin-Pintueles, Laurent Galineau, Lydie Nadal-Desbarats, Camille Dupuy, Sylvie Bodard, Julie Busson, Antoine Lefèvre, Patrick Emond, Sylvie Mavel

► **To cite this version:**

Alexandra Bourdin-Pintueles, Laurent Galineau, Lydie Nadal-Desbarats, Camille Dupuy, Sylvie Bodard, et al.. Maternal Rat Metabolomics: Amniotic Fluid and Placental Metabolic Profiling Workflows. *Journal of Proteome Research*, 2021, 20 (8), pp.3853-3864. 10.1021/acs.jproteome.1c00145 . hal-03954760

HAL Id: hal-03954760

<https://hal.science/hal-03954760>

Submitted on 10 Nov 2023

HAL is a multi-disciplinary open access archive for the deposit and dissemination of scientific research documents, whether they are published or not. The documents may come from teaching and research institutions in France or abroad, or from public or private research centers.

L'archive ouverte pluridisciplinaire **HAL**, est destinée au dépôt et à la diffusion de documents scientifiques de niveau recherche, publiés ou non, émanant des établissements d'enseignement et de recherche français ou étrangers, des laboratoires publics ou privés.

Maternal rat metabolomics: amniotic fluid and placental metabolic profiling workflows

Alexandra Bourdin-Pintueles ¹, Laurent Galineau ¹, Lydie Nadal-Desbarats ¹, Camille Dupuy ¹,
Sylvie Bodard ¹, Julie Busson ¹, Antoine Lefèvre ¹, Patrick Emond ^{1,2}, and Sylvie Mavel ^{*1}

¹ *UMR 1253 iBrain, Université de Tours, Inserm, Tours, France*

² *CHRU de Tours, Service de Médecine Nucléaire In Vitro, Tours, France*

* Corresponding author:

Sylvie Mavel - *UFR Médecine, INSERM U1253, Eq IBT, 10 Bd Tonnellé, 37000 Tours, France-*

tel :+(33)247366279 – e-mail: mavel@univ-tours.fr

Abstract

Studying the metabolome of specific gestational compartments is of growing interest in the context of fetus developmental disorders. However, the metabolomes of the placenta and amniotic fluid (AF) are poorly characterized. Therefore, we present the validation of a fingerprinting methodology. Using pregnant rats, we performed exhaustive and robust extractions of metabolites in the AF and, lipids and more polar metabolites in the placenta. For the AF, we compared the extraction capabilities of methanol (MeOH), acetonitrile (ACN), and a mixture of both. For the placenta, we compared (i) the extraction capabilities of dichloromethane, methyl *t*-butyl ether (MTBE), and butanol, along with (ii) the impact of lyophilization of the placental tissue. Analyses were performed on a C18, and hydrophilic interaction liquid chromatography combined with high-resolution mass spectrometry (LC-HRMS). The efficiency and the robustness of the extractions were compared based on the number of the features or metabolites (for untargeted or targeted approach, respectively), their mean total intensity, and their coefficient of variation (%CV). The extraction capabilities of MeOH and ACN on the AF metabolome were equivalent. Lyophilization had also no significant impact and usefulness on the placental tissue metabolome profiling. Considering the placental lipidome, MTBE extraction was more informative because it allowed extraction of a slightly higher number of lipids, in higher concentration. This proof-of-concept study assessing the metabolomics and lipidomics of the AF and the placenta revealed changes in both metabolisms, at two different stages of rat gestation, and allowed a detailed prenatal metabolic fingerprinting.

Keywords: LC-MS, NMR, targeted, untargeted, lipidomics, fingerprinting methodology, validation, pregnant rodent

Abbreviations

AF, Amniotic fluid; BuMe, Butanol/methanol; FDR, false discovery rate; GD13, gestational day 13; GD19, gestational day 19; MTBE, methyl tert-butyl ether; NUS, non-uniform sampling.

1. INTRODUCTION

Metabolomics allows for the detection, identification, and quantification of small molecules (below 1 kDa) like amino acids, hormones, and sugars in human, animal, vegetal, and cell samples. The amount of those compounds, called the metabolome, reflects the metabolism of the organism as they represent substrates, intermediates and products of multiple biochemical pathways. Thus, metabolomics is increasingly used for biomarkers discovery, establishing pathophysiological metabolome signatures, and used in diagnosis, pharmacological treatment research, and toxicological studies.¹ Metabolomics studies have been optimized on several matrices such as urine, serum/plasma, or feces samples.² However, specific pathophysiological contexts require investigating other matrices. To date, there is a growing interest for using metabolomics in the context of neurodevelopmental disorders to find biomarkers for an early diagnosis.³⁻⁴ In this context, metabolomics of other matrices at the interface between the mother and the developing child such as amniotic fluid (AF)⁵ and placenta^{4,6} is of a great interest but still poorly documented.⁷ In fact, the metabolism of AF reflects the physiological processes of fetal development⁸⁻⁹ and as an interface between the mother and the fetus, the placenta performs multiple functions to support pregnancy functions and a normal fetal development.¹⁰ Altogether, this makes the metabolomics of placenta and AF an extremely valuable material for fetal health diagnostics.

Several studies have explored the metabolome of the AF^{5, 11-14} and the placenta.¹⁵⁻¹⁷ However, there is still a lack of information related to their characterization, and on the best suited methodology to study these matrices. Our objective was to develop an exhaustive and robust method to study the AF and placental metabolomes along with the placental lipidome using pregnant rat samples to obtain a global profiling of these two compartments. We investigated the AF metabolome using three solvent extraction protocols analyzed by (i) ultra-

high liquid chromatography with high-resolution mass spectrometry (UHLC-HRMS) with two chromatographic columns, C18- and hydrophilic interaction liquid chromatography (HILIC), and (ii) nuclear magnetic resonance (NMR). Regarding the placenta, the impact of working on frozen or lyophilized samples was investigated as well as three solvent extractions were compared. The lipidomics (study of lipid metabolism) was performed using reverse phase-liquid chromatography with mass spectrometry (RP-LC-MS), and from this extraction, the more polar metabolome was investigated by C18- and HILIC-LC-MS. In addition to the multiplatform analyses, a targeted and a non-targeted approach were both used in order to expose a global view of the metabolome of these matrices, according to the extracting solvents tested, in order to meet the expectations of the metabolomics researchers.

Finally, a proof-of-concept study was performed using the defined optimal conditions to study the evolution and complementarity of the AF and placental metabolomes at two gestational stages. Gestational stage 13 and 19 correspond to late embryonic and fetal stages in rats, respectively.¹⁸ These two gestational time points were chosen to observe modifications in the metabolisms of maternal and fetal matrices during these two key periods of gestation as potential tools for biological studies.

2. EXPERIMENTAL SECTION

2.1. *Animals*

All animal experiments were conducted in accordance with local and international guidelines and approved by a local ethics committee. Fourteen pregnant female Wistar rats were purchased (Janvier Labs, Le Genest St. Isle, France) and were individually housed under

humidity- and temperature-controlled conditions and a 12:12 light-dark cycle (light on at 7.00 AM) with access to food and water *ad libitum*. Rats were randomly distributed into 2 groups of 7 females: GD13 group and GD19 group, corresponding to the day of sacrifice by decapitation at 13 and 19 gestational days, respectively. Each female had between 10 and 12 fetuses.

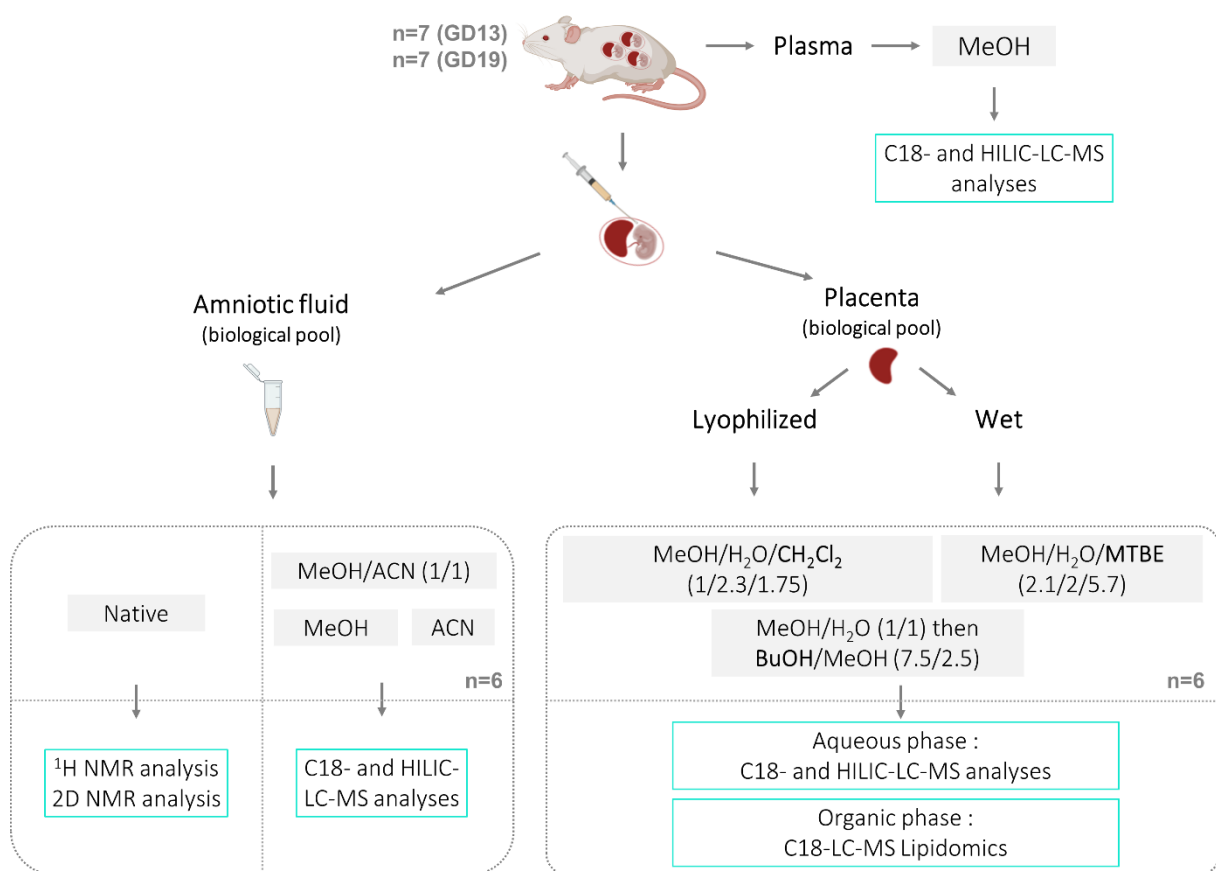


Figure 1: Workflow protocol for optimization of amniotic fluid and placenta preparation, extraction and analytical processes.

2.2 Sample collection and storage

Blood (1 mL) was collected from each female after decapitation in a 1.5 mL Eppendorf tube containing 1.8 mg/mL of ethylenediaminetetraacetic acid (EDTA), centrifuged at 5,000 xg

during 20 minutes at 4°C, and stored at -80°C. After cesarean section, the AF of each gestational sac was collected with a 1-mL syringe and a 26-gauge needle, pooled into two 1.5 mL Eppendorf tubes (to give a biological pool used for all the experiments), and stored at -80°C. The placenta of each gestational sac was also collected, rinsed with saline, pooled into two 1.5 mL Eppendorf tubes, and stored at -80°C.

2.3. UHPLC-HRMS analyses

2.3.1. Amniotic fluid

Metabolites were extracted with three different methods. AF (150 µL of the biological pool) were mixed with 20 µL of internal standards (IS) (a mixture of 7 drugs: fenofibrate, sulfapyridine secobarbital, phenobarbital, cethexonium bromide, promethazine, and sulfanilamide) and 400 µL of either methanol (MeOH), acetonitrile (ACN), or methanol/acetonitrile (1:1) (n = 6 replicates each). Samples were vortexed for 5 seconds, and incubated at -20°C during 30 minutes. Then, samples were centrifuged at 5,000 xg at 4°C during 15 min, and 410 µL of supernatant was retrieved. A second extraction was performed, and the cumulative 820 µL collected was equally subdivided in half for future C18 and HILIC analyses, evaporated at 40°C using a SpeedVac Concentrator and stored at -80°C until LC-MS analysis. Then, the best protocol was tested on 7 individually collected samples at GD13 and GD19.

2.3.2. Placenta

For placental tissue, we compared 3 extraction methods on either wet or lyophilized tissue. Frozen placenta pool was homogenized with an Ultra Turax (Ika, Staufen, Germany) at 20,000 rpm 5 minutes. Then 18 x 40 mg were weighed in Eppendorf tubes and stored at -80°C until extraction. The remainder was lyophilized during 48 hours in a FreeZone[®] lyophilizer (Labconco, Kansas City, MO, USA). From the resulted fine powder, 18 x 6 mg (corresponding to approximately 40 mg of wet tissue) were weighed in Eppendorf tubes followed by the extraction process.

The modified Bligh-Dyer, Matyash and Butanol/Methanol (BUME) methods were tested to extract both metabolome and lipidome.

A) 1 mL of MeOH/H₂O (milli-Q) (1:1) (n = 6 replicates each) was added to 40 mg of wet tissue, or to 6 mg of lyophilized tissue. Samples were vortexed 2 minutes, incubated 20 minutes at -20°C , supplemented with 340 μL of dichloromethane (CH₂Cl₂), and 30 μL of a solution of IS. CH₂Cl₂ was used instead of chloroform due to its lower toxicity and its similar properties.¹⁹ After homogenization, samples were centrifuged at 5,000 xg at 4°C for 15 minutes. The upper phase (660 μL) was removed and kept in vials. Then, a second extraction with 990 μL of CH₂Cl₂/ACN/H₂O (milli-Q) (1:1:1) was performed. The upper phase (400 μL) was removed, added to the precedent 660 μL , and then equally separated for future C18 and HILIC analyses, while the lower phase was put into vials for lipidomics analysis.

B) 330 μL of MeOH (n = 6 replicates each) was added to 40 mg of wet tissue or 6 mg of lyophilized tissue. Samples were vortexed 2 minutes, incubated at -20°C for 20 minutes, supplemented with 1.2 mL of methyl tert-butyl ether (MTBE)/H₂O (milliQ) (2:1), and 30 μL of IS. After homogenization, samples were centrifuged at 5,000 xg at 4°C for 15 minutes. The upper phase (600 μL) was removed and kept for lipidomics analysis. A second extraction with

900 μL of MTBE/MeOH/H₂O (milli-Q) (6:2:1) was performed. The upper phase (400 μL) was removed and added to the previous 600 μL , while the lower phase was equally separated for C18 and HILIC analyses.

C) 500 μL of MeOH/H₂O (milli-Q) (1:1) and 30 μL of IS (n = 6 replicates each) were added to 40 mg of wet tissue, or 6 mg of lyophilized tissue. Samples were vortexed for 2 minutes, incubated at -20°C for 20 minutes, and centrifuged at 5,000 xg at 4°C for 15 minutes. The supernatant (400 μL) was collected into vials. A second extraction with 1 mL of MeOH/H₂O (milli-Q) (1:1) was performed. The supernatants (800 μL) were added to the precedent 400 μL , and then subdivided for future C18 and HILIC analyses. Then, 500 μL of BuOH/MeOH (milli-Q) (0.75:0.25) was added to the pellet to extract lipids. After homogenization, samples were centrifuged at 5,000 xg at 4°C for 15 minutes, and the supernatant (300 μL) was collected into vials. A second extraction was performed and 300 μL of supernatant was added to the first ones for lipidomics analysis. Samples were evaporated at 40°C using a SpeedVac Concentrator and stored at - 80°C until LC-MS analysis.

2.3.3. Plasma

Plasma (50 μL) was mixed with 20 μL of IS and 400 μL of cold MeOH, vortexed for 5 seconds and incubated 30 minutes at 4°C. Samples were centrifuged at 5,000 xg during 25 minutes at 4°C. The supernatant (350 μL) was equally subdivided in half for future C18 and HILIC analyses, samples were evaporated at 40°C using a SpeedVac Concentrator and stored at - 80°C until LC-MS analysis.

2.3.4. UHPLC-HRMS parameters

The aqueous fractions of AF, placenta and plasma were reconstituted with 100 μL of H_2O (milli-Q)/MeOH (9:1) for C18, and 100 μL of ACN/ H_2O (milli-Q) (9:1) for HILIC. The liposoluble fractions of the placenta were reconstituted with 100 μL of a 6:3:1 mix of ACN/ H_2O /isopropanol before LC-MS. LC-MS analysis was performed as previously described.²⁰⁻²¹ Briefly, a UHPLC Ultimate 3000 system (Dionex, Sunnyvale, CA, USA), coupled to a Q-ExactiveTM quadrupole-orbitrap-MS (Thermo Fisher Scientific, San Jose, CA, USA) was operated in positive electrospray ionisation (ESI+) and negative electrospray ionisation (ESI-) mode. For C18-LC-MS analysis, chromatography was carried out with a 1.7 μm C18-XB (150 mm \times 2.10 mm, 100 \AA) UHPLC column (Kinetex, Phenomenex, Torrance, CA, USA) heated at 55°C. The solvent system comprised mobile phase A (H_2O + 0.1% formic acid), and mobile phase B (MeOH + 0.1% formic acid); the gradient operated at a flow rate of 0.4 mL/min over a run time of 26 min. The multi-step gradient was programmed as follows: 0 to 6 minutes, 99.9% A; 6 to 10 minutes, 75% A; 10 to 12 minutes, 20% A; 12 to 14 minutes, 10% A; 14 to 17 minutes, 0.1% A; 17 to 20 minutes, 99.9% A; 21 to 24 minutes, 99.9% A. For HILIC-LC-MS analysis, chromatography was carried out with a 1.7 μm Cortecs HILIC-virgin silica (150 mm \times 2.10 mm, 100 \AA) UHPLC column (Waters) heated at 40°C. The solvent system comprised mobile phase A (H_2O + 0.5% formic acid + 10 mM ammonium formate), and mobile phase B (ACN + 0.5% formic acid + 10 mM ammonium formate); the gradient operated at a flow rate of 0.4 mL/min over a run time of 23 minutes. The multi-steps gradient was programmed as follows: 0 to 8 minutes, 5% A; 8 to 15 minutes, 18% A; 15 to 15.5 minutes, 25% A; 15.5 to 16 minutes, 75% A; 16 to 18.1 minutes, 97% A; 18.1 to 23 minutes, 5% A. For lipidomics analysis, chromatography was carried out with a 1.7 μm Kinetex C18 (150 mm \times 2.10 mm, 100 \AA) UHPLC column (Phenomenex) heated at 55°C. The solvent system comprised mobile phase C

(Isopropanol/ACN (9:1) + 0.1% (v/v) formic acid + 10 mM ammonium formate), and mobile phase D (ACN/H₂O (6:4) + 0.1% (v/v) formic acid + 10 mM ammonium formate); the gradient operated at a flow rate of 0.260 mL/min over a run time of 30 minutes. The multi-steps gradient was programmed as follows: 0 to 1.5 minutes, 32% C; 1.5 to 5 minutes, 45% C; 5 to 8 minutes, 52% C; 8 to 11 minutes, 58% C; 11 to 14 minutes, 66% C; 14 to 18 minutes, 70% C; 18 to 21 minutes, 75% C; 21 to 24 minutes, 97% C; 24 to 30 minutes, 32% C. The autosampler temperature (Ultimate WPS-3000 UHPLC system, Dionex) was set at 4°C, and the injection volume for each sample was 5 µL. During the full-scan acquisition, which ranged from 250 to 1600 *m/z*, the instrument operated at 70,000 resolution.

The instrumental stability was evaluated by multiple injections (*n* = 5) of a quality control (QC) sample obtained from a pool of 10 µL of all samples of one matrix. This QC sample was injected at the beginning of the analysis, between every 10 sample injections, and at the end of the run.²²⁻²³ Two diluted QC samples dilutions (to 1/2 and to 1/4) were studied to determine the linearity of the dilution curves, showing the robustness of a metabolite analysis. A blank was injected at the beginning, and at the end of the run.²⁴

2.4. NMR

NMR 1D was done as previously described.²⁵ Briefly, a pool of AF was thawed, and 150 µL (or 100 or 50 µL for robustness study through analysis of the linearity of dilution curves) was added *qsp* 200 µL of 0.2 M potassium phosphate buffer in deuterium oxide (D₂O) 99%. Eight µL of 3-trimethylsilylpropionic acid (0.05 wt% in D₂O) were added to samples as an internal reference. After centrifugation, the supernatant was transferred to 3-mm NMR tubes. The NMR spectra were obtained with a BrukerDRX-600 AVANCE-III HD spectrometer (Bruker

SADIS, Wissembourg, France), operating at 14 T, with a TCI cryoprobe (Bruker SADIS). ^1H -NMR spectra were acquired using a “noesypr1d” pulse sequence with a relaxation delay of 10 seconds. ^1H spectra were collected with 128 scans. A “Hsqcetgp” pulse sequence for 2D (^1H - ^{13}C) NMR was used with 4096 x 256 data points using 64 scans per increment, with a relaxation time of 2.5 seconds. Resolution-enhanced spectra were done, without loss of sensitivity, using a non-uniform sampling (NUS) approach. NUS spectra are faster to acquire than conventional ones,²⁶ in our case 3 hours.

2.5. *Data processing*

2.5.1. *LC-MS*

For the LC-MS targeted approach, a library of 495 standard compounds (Mass Spectroscopy Metabolite Library of Standards MSMLSTM, IROA TechnologiesTM) was analyzed with the same gradient of mobile phases and in the same conditions than those used for this study. In order to validate the identity of detected metabolites, the retention time must be within 6-20 seconds of the standard reference, the measured molecular mass of the metabolite must be within 10 ppm of the known mass of the reference compound and the isotope ratios of the metabolite must match the standard reference. The signal was calculated using Xcalibur software (Thermo Fisher Scientific) by integrating selected ion chromatographic peak area.

For the untargeted approach, data were analyzed using Workflow4Metabolomics (W4M) an online platform including XCMS.²⁷ A pre-processing workflow was created in our laboratory following the global steps: 1) CentWave-chromatographic peak detection with a max tolerated ppm m/z deviation of 15.0 and a minimum difference in m/z of 0.008 for the extraction method, 2) alignment method by grouping chromatographic peaks within and

between samples by PeakDensity with a bandwidth of 10 and by using Obuwrap for the retention time correction. Only $[M+H]^+$ ion was kept for the further analysis.

Only metabolites/features detected in 80% of repetitions were kept for the further analysis. Data were normalized to the total area of peaks of interest, metabolites and lipids with CV > 30% in QC and not respecting the dilution law were ejected.²⁴ The list of the annotated metabolites is given in Supporting Information (Table S1).

2.5.2. NMR

Data were analyzed as previously described²⁸. NMR spectra were processed using TopSpin version 3.6.1 software (Bruker Daltonik, Karlsruhe, Germany). Identification of metabolites was achieved using Chenomx software (Chenomx Inc, Edmonton, Canada). 2D spectra were processed using MestReNova version 7.1.0 software (Mestrelab Research, Santiago de Compostela, Spain) as previously described.²⁹ The signals were assigned using the Metabominer software³⁰ with tolerances of 0.05 ppm (^1H) and 0.1 ppm (^{13}C).

2.5.3. Statistical analysis

The coefficient of variation (%CV) was calculated as the ratio of the standard deviation to the mean, and multiplied by 100. Non-parametric tests (Wilcoxon rank-sum test) were obtained from Metaboanalyst web site (www.metaboanalyst.ca), the false discovery rate (FDR) corrected p values were provided.³¹ Unsupervised multivariate analysis [principal components analysis (PCA)] was done as previously described using Simca-P+-15 software (Umetrics, Umeå, Sweden).³² Venn diagrams were performed using the free software Hello jvenn!.³³

3. RESULTS AND DISCUSSION

A targeted approach will be preferred if the aim of the study concerns a group of metabolites, e.g. amino acids, neurotransmitters, or others. A non-targeted approach will be favored to determine if there is a change in metabolome between various conditions and will then guide a possible targeted approach. Results were analyzed using both targeted and untargeted approaches. The aim of targeted metabolomics is to quantify specific molecules, while untargeted metabolomics aims at screening a maximum of metabolites and identifying the ones that are the most discriminant between several conditions. In LC-MS, due to the physicochemical properties of LC columns, the less polar compounds are mainly retained on a RP-C18 column, while many polar metabolites are eluted near the void volume. The polar compounds are generally retained on a HILIC column, but this chromatography could optionally lead to less reproducible untargeted metabolic profiling and requires longer equilibration time than RP-LC-MS. As no single chromatographic method is ideal to detect all classes of metabolites, the combination of both columns will extend the range of detected molecules in a biological sample.

3.1. Optimization of extraction

3.1.1 Amniotic fluid

The AF metabolome has been frequently studied using NMR in clinical and preclinical studies,^{11, 34} but for the past few years, the use of LC-MS is quickly increasing.³⁵ Several studies already report the use of different solvent like MeOH or ACN to deproteinize and extract metabolites,^{12, 17, 36} but without a rationale for their choice. We have so assessed three extraction methods using MeOH, ACN or a mixture of both solvents on rat AF samples.

3.1.1.1. LC-MS analysis

Targeted analysis

Table 1: Reproducibility assesment of metabolites detected in AF in C18 and HILIC LC-MS targeted analyses in ESI+/- modes (n = 6 replicates).

Amniotic fluid – Targeted analysis	MeOH		ACN		MeOH/ACN	
	C18 ESI+/-	HILIC ESI+/-	C18 ESI+/-	HILIC ESI+/-	C18 ESI+/-	HILIC ESI+/-
Mean total intensity (standard deviation)	1.45E+10 (4.5E+08)	6.16E+09 (2.3E+08)	1.34E+10 (3.7E+08)	3.83E+09 (1.6E+08)	1.33E+10 (9.9E+08)	7.34E+09 (1.5E+09)
Total metabolites	197	170	193	162	195	165
Number of reproducible metabolites (CV<30%)	167	139	167	122	157	108
Mean of %CV from reproducible metabolites	8.5	11.6	8.5	13.7	7.7	16.5

The solvent extraction efficiency was evaluated through two approaches: *via* the total intensity of the extracted features and *via* the total number of extracted metabolites. In the C18-LC-MS platform, the mean total intensities of all targerted extracted metabolites with MeOH was 8% higher than with ACN and MeOH/ACN extractions; ACN and MeOH/ACN were equivalent. The same trend was observed for reproducible metabolites (with a CV < 30%)³⁷

(Table 1). The same results were obtained with the untargeted approach (Table 2). These mean intensities were globally 66% higher than with HILIC-LC-MS platform. Using HILIC-LC-MS, the efficiency of the MeOH extraction was 40% higher than the ACN extraction and was 1% lower than the MeOH/ACN extraction (Table 1).

The total number of metabolites detected in rat AF depended on the solvent for extraction, and their specificity was investigated in targeted analysis (Figure 2). Interestingly, the 3 solvents were roughly equivalent in regard to the total number of metabolites extracted (Figure 2A), as 81% to 83% of metabolites were commonly detected with each method. Among the 416 metabolites detected regardless of the solvent used for extraction, MeOH was the solvent leading to the highest number of metabolites detected (367) (Figure 2A).

The quality of each extraction was evaluated by the repeatability based on PCA (Supporting Information, Figure S1) and %CV. For the 3 solvents used, the C18-LC-MS platform detected the highest number of reproducible metabolites (with a CV < 30%) compared to the HILIC-LC-MS platform (Table 1). With the C18-LC-MS platform, the number of reproducible metabolites extracted by MeOH and ACN were equal (167 among 197 annotated metabolites) and slightly lower for MeOH/ACN extraction (157 among 195 annotated) (Table 1), leading to similar total intensities of targeted metabolites with a CV < 30% compared to the total intensity of all metabolites (Table 1). With the HILIC-LC-MC platform, MeOH extracted a higher number of reproducible metabolites (139) compared to 122 reproducible metabolites with ACN extraction and 108 with the mixture of both solvents (Table 1). Among the replicable metabolites extracted with MeOH, 72 % were column-specific, and 28 % were detected using both columns (Figure 2B). These results highlight the importance of combining RP and HILIC chromatography columns for a better metabolome coverage . A list of metabolites detected

in AF with MeOH extracting solvent regarding the column and ionisation mode is in the Supporting Information (Table S1).

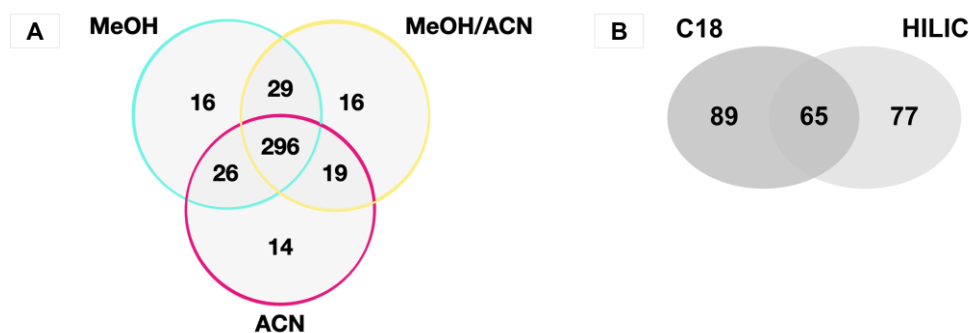


Figure 2: Amniotic fluid analysis using targeted C18 and HILIC LC-MS (ESI+ /- modes) (n = 6 replicates) (A) Total number of metabolites detected depending on the extraction solvent: MeOH, ACN or a mixture of both; (B) Complementarity of reversed-phase (RP-C18) and HILIC LC-MS from MeOH extraction.

Fetal metabolism contributes to the composition of AF, which changes during gestational stages due to fetal swallowing and lung, urine and gastric fluid releases. From a MeOH extraction, after a data processing (we kept molecules with a CV < 30% in the QC and must respect of the dilution law), 200 unique robust metabolites among 495 molecules of our target library were annotated. About 31 % of robust annotated compounds in AF, belong to the amino acids or derivatives family, followed by 24 % of aromatic compounds and vitamins, and 15 % of simple lipids like fatty acids, steroids and hormones (Figure 3).

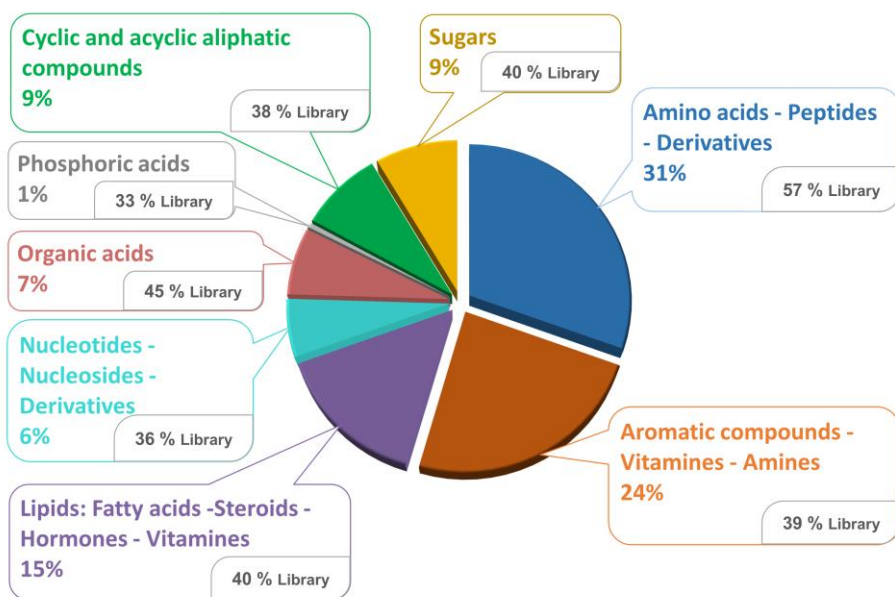


Figure 3: Chemical classes of robust annotated compounds in AF, extracted with MeOH, and the percentage of the detected compounds relative to the number of metabolites in our library, for each class.

Untargeted analysis

The results were similar in the untargeted approach. Using the C18-LC-MS platform, by untargeted approach, the extraction efficiencies using the total number of features detected were equivalent with each extraction method in ESI+ and ESI- modes (around 3,000 and 1,960 features, respectively) (Table 2). Considering the reproducible features (with a CV < 30%) of the C18-LC-MS (ESI+) platform, MeOH was a little bit more effective (+48 *versus* +111 features for ACN *versus* MeOH/ACN extraction methods, respectively), and yielded the highest integrated intensity (+ 12% *versus* ACN; + 9% *versus* MeOH/ACN). In HILIC-LC-MS (ESI+), around 4450 features were detected with MeOH, providing +910, and +645 reproducibles features compared to ACN and MeOH/ACN extractions, respectively. The same

trend was observed in ESI- mode (Table 2). The numbers of metabolites extracted with MeOH and ACN were similar to those found in the literature for human AF.^{12, 36} The 3 solvents showed a similar reproducibility in targeted C18-LC-MS with a mean %CV of 8%. Using the untargeted approach, the global reproducibility was similar for the 3 solvents and was higher using the C18-LC-MS analysis compared to the HILIC-LC-MS analysis (CV = 12-14% and 17-21%, respectively).

In conclusion, with regards to extraction efficiency and reproducibility, MeOH and ACN were almost similar. According to specific uses (e.g. only one column, only one approach (targeted/non-targeted), or only one ionisation) the choice of the solvent (MeOH versus ACN) could be done based on the different tables provided in this study. Taking in account both approaches, both columns, and both ionisations, MeOH was slightly more effective and was therefore chosen for the application experiment described in section 3.2.

Table 2: Reproducibility assesment of metabolites detected in AF in C18 and HILIC LC-MS using untargeted analyses in ESI+/- modes (n = 6 replicates).

Amniotic fluid - Untargeted analysis		MeOH		ACN		MeOH/ACN	
		C18	HILIC	C18	HILIC	C18	HILIC
Mean total intensity (standard deviation)	ESI+	2.32E+10	1.26E+10	2.12E+10	7.58E+09	2.33E+10	7.34E+09
		(5.8E+08)	(8.4E+08)	(7.9E+08)	(1.0E+09)	(7.9E+08)	(1.3E+09)
	ESI-	9.30E+09	8.83E+09	8.50E+09	9.35E+09	9.06E+09	1.05E+10
		(2.8E+08)	(6.6E+08)	(4.7E+08)	(8.9E+08)	(3.9E+08)	(7.4E+08)
Total features	ESI+	3020	4400	3005	4482	3020	4473
	ESI-	1958	3599	1961	3621	1960	3635
Features with	ESI+	1725	1182	1677	2092	1614	1447

CV < 30%	ESI-	1374	1697	1322	1577	1376	1247
Mean %CV from reproducible features	ESI+	13.8	18.4	14.9	20.0	14.3	21.5
	ESI-	12.7	18.0	14.7	18.9	13.0	20.4

3.1.1.2. NMR

Based on the excellent reproducibility of NMR (e.g. for longitudinal studies), its quantitative accuracy of the analyzed metabolites (e.g. a single internal reference is sufficient for absolute metabolite quantitation over a huge range of concentration), and its ability to identify structures, NMR 1D (^1H) completed by 2D analysis is of a great interest for the metabolome characterization.³⁸ From native rat AF samples, 41 metabolites were detected in 1D NMR, and 5 additional metabolites were detected by 2D (these compounds were non-assigned by ^1H due to compound overlapping: *O*-phosphoethanolamine, serine, arginine, phosphocholine, and taurine (Supporting Information, Table S2). We performed a resolution-enhanced 2D NMR by using non-uniform sampling (NUS), with no increase in experimental time.²⁶ Heteronuclear single quantum coherence spectroscopy (HSQC) NMR (Figure 4) provided 34 assignments corresponding to aliphatic compounds, aromatic metabolites could not be observed at 600 MHz even after 3 hours of accumulation. For an analytical comparison, Graça and colleagues described in human AF (but from 1 mL) around 50 molecules detected at 800 MHz.¹¹ While 18 of these molecules were not observed in our analytical conditions, we annotated 12 other molecules that they were not described in their analysis (see comparison in Table S2, Supporting Information). From the 1D NMR analysis, 91% of the detected molecules were robust, while 14 molecules did not follow a linear dilution curve (from 150,

100, and 50 μL samples). One of the major assets of NMR is to provide simultaneous quantification of routine metabolites. An example of quantification of several rat AF metabolites can be found in the supplementary data (Figure S2). The complementarity of LC-HRMS (C-18 + HILIC, 200 unique metabolites) and NMR (1D + 2D, 46 molecules) showed 19 metabolites analyzed only by NMR (Supporting Information, Figure S3).

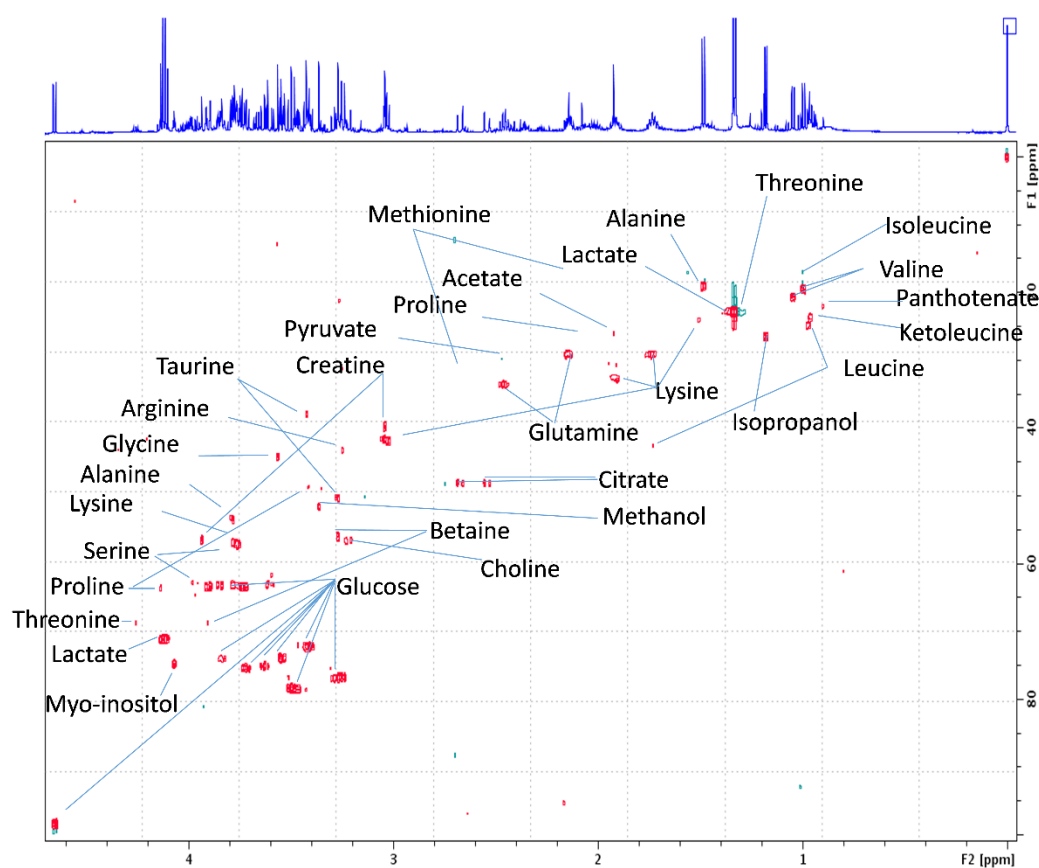


Figure 4: 1D (^1H) NMR and 2D heteronuclear (HSQC) spectra of rat amniotic fluid sample (150 μL) at 600 MHz and assignment.

3.1.2. Placenta

Due to the high lipid content of the placenta, biphasic extractions such as the Folch method or the Bligh-Dyer method,^{22, 39} and the Matyash method¹⁷ have been performed to collect

both the metabolome and lipidome. BuOH/MeOH (BuMe) extraction has been used for plasma lipidomics⁴⁰ but has been rarely tried with tissue samples. Few papers described BuMe as an extraction solvent for placenta tissue,⁴¹ and it has not been used for the extraction of both metabolome and lipidome. Therefore, we compared CH₂Cl₂/MeOH, MTBE/MEOH and BuMe as solvent extractions for both metabolome and lipidome characterizations.

Lipidomics

Table 3: Reproducibility assesment of lipids detected in wet or lyophilized placenta in LC-MS (ESI+/- modes) (targeted analyses) (n = 6 replicates).

Placenta Lipidomics - Targeted analysis (ESI+/-)	CH ₂ Cl ₂		MTBE		BuOH	
	Wet	Lyoph	Wet	Lyoph	Wet	Lyoph
Mean total intensity (standard deviation)	9.37E+09 (3.2E+09)	5.01E+09 (8.3E+09)	2.21E+10 (1.6E+09)	2.45E+10 (5.9E+09)	9.55E+09 (2.3E+09)	8.15E+09 (2.6E+09)
Total lipids	247	227	281	277	249	250
Mean of %CV from lipids with CV<30%	20.9	19.8	21.1	21.7	22.1	19.5

Regarding lipidomics, our results showed that working on fresh or lyophilized placenta was almost equivalent in regard to total intensity, quantity of lipids extracted, and reproducibility (%CV), regardless of the solvent used. Indeed, 94 ± 4% of the lipids extracted were observed using both types of samples (Table 3, Figure S4, Supporting Information). In parallel, the multivariate analysis by PCA revealed that the major difference came from the choice of the

extracting solvent (MTBE versus BuOH and CH₂Cl₂) (PC1=0.58), the lyophilization was much less impactful (Supporting Information, Figure S5).

Using untargeted lipidomics analysis, wet or lyophilized tissue gave the same results when extracted using MeOH or BuOH (Figure 5A, Table S4), but MTBE extraction on wet tissues was slightly more effective with more features detected compared to lyophilized tissue in both targeted and untargeted studies (Figure 6, Table S4). MTBE extraction also led to higher intensities of lipids than CH₂Cl₂ and BuOH extractions (Table 3, Figures 5 and 6).

Contrary to CH₂Cl₂, MTBE is the upper phase in the biphasic extraction step, which is an important advantage in the experimental process. This could explain the higher robustness of the extraction on wet placenta (68% of robust lipids (with a CV < 30%) compared to 61% (but 10 time less intense) using CH₂Cl₂ and 41% and BuOH, respectively.

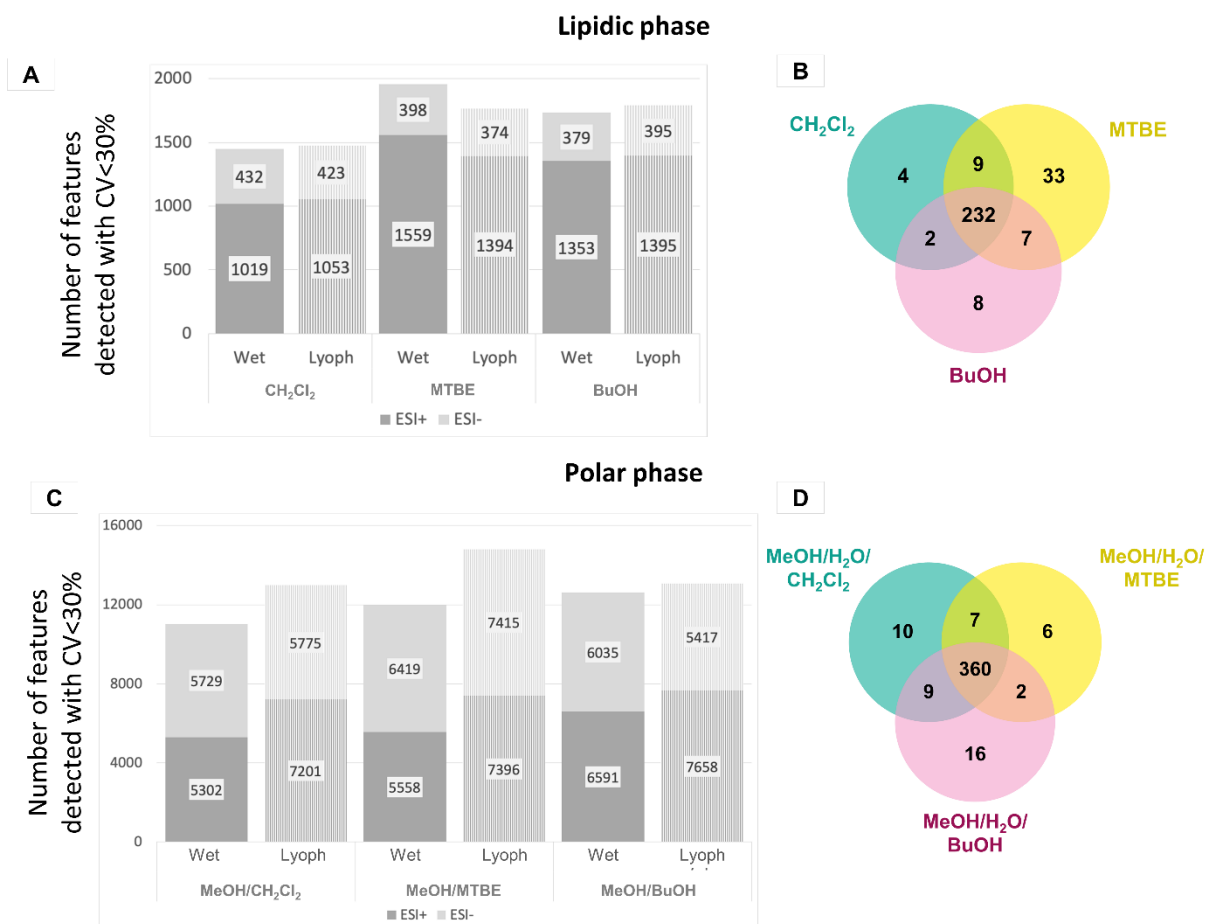


Figure 5: LC-MS analyses (ESI+ and ESI-) of wet placenta for each lipidome/metabolome extraction solvent: MeOH/CH₂Cl₂, MeOH/MTBE, MeOH/BuOH, (n = 6 replicates). (A) Total number of detected lipidic features; (B) Specificity of the extracting solvent on the number of targeted lipids; (C) Total number of detected features; (D) Specificity of the extracting solvent on the number targeted metabolites.

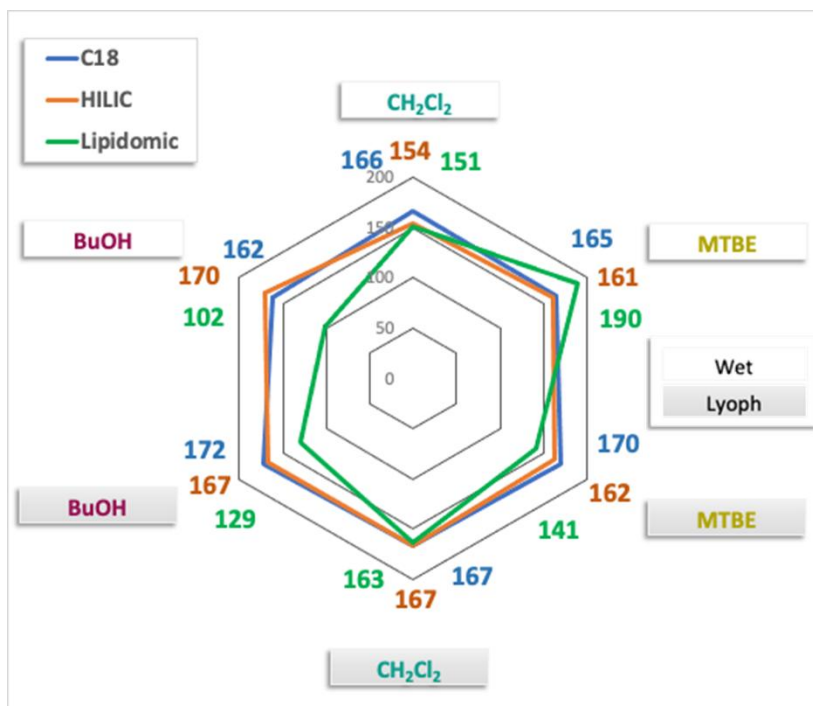


Figure 6: Number of polar metabolites and lipids detected in placenta using C18 and HILIC LC-MS analyses and lipids in ESI+ and ESI- modes with a CV < 30 % for each extraction solvent: CH₂Cl₂, MTBE or BuOH (targeted analysis) (n = 6 replicates).

Table 4: Reproducibility of detected metabolites in wet or lyophilized placenta by C18 and HILIC LC-MS targeted analyses (ESI+/- modes), extracted using MeOH/H₂O/MTBE (n = 6).

Placenta metabolomics - Targeted analysis		MeOH/H ₂ O/MTBE	
		Wet	Lyoph
Mean total intensity (standard deviation)	C18 ESI+/-	1.86E+10 (1.6E+09)	1.94E+10 (7.0E+08)
	HILIC ESI+/-	7.53E+10 (5.4E+09)	7.42E+10 (1.3E+09)
Total metabolites	C18 ESI+/-	189	192
	HILIC ESI+/-	186	184
Mean %CV from reproducible metabolites	C18 ESI+/-	13.3	8.8
	HILIC ESI+/-	13.2	10.2

Polar metabolomics

Regarding the metabolome, HILIC and C18 LC-MS provided similar results in terms of intensities and number of detected metabolites for wet or lyophilized placentae as observed by Troisi and collaborators.⁴² Furthermore, no notable impact of the lipid solvent extraction was detected as the 3 protocols led to the same metabolome (Table 4, Figure 5, Table S3 in Supporting Information). Regarding the detection coverage, from a MeOH/H₂O/MTBE extraction, after a drastic data processing (CV < 30% in the QC and the respect of the dilution law), about 32 % of robust annotated metabolites in placenta belong to amino acids or derivatives, 21 % to aromatic compounds and vitamins, and 14 % to small lipids like fatty acids and hormones. The repartition of the different chemical classes of annotated placenta metabolome was similar to what we observed in AF (Figure 3).

Considering the efficiency, reproducibility, and the time needed for lyophilization, a biphasic extraction with MTBE on wet placenta was chosen for the rest of the experiment (see section 3.2).

3.2. Application: Study of 2 gestational stages

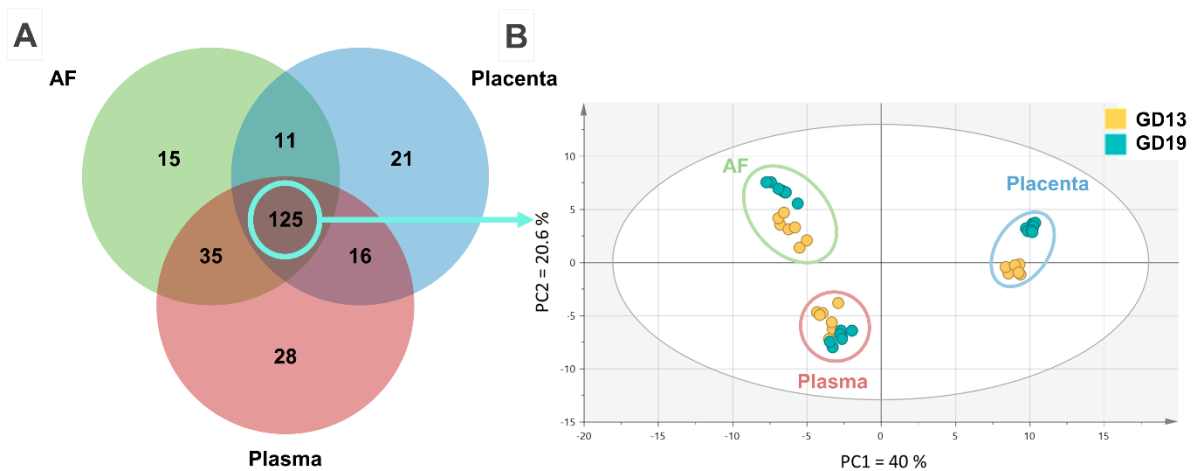


Figure 7: (A) Complementarity of common metabolites detected between AF, placenta, and plasma. (B) Score plot of the principal component analysis of AF, placenta and plasma at GD13 and GD19 stages, from the 125 common detected metabolites in the 3 matrices ($n = 7$ females): $R2X(\text{cum})=0.88$, $Q2(\text{cum})=0.81$.

As a proof of concept, the metabolomes of AF and placenta, ($n = 7$ pregnant rats per group), were compared at two gestational stages, gestational day 13 (GD13) and gestational day 19 (GD19), corresponding to the second month and end of the first trimester of pregnancy in human, respectively.¹⁸

To complete the specific maternal compartment metabolic fingerprinting, we also analyzed the plasma profiling to evaluate the complementarity of these different matrices. For each matrix, the number of detected targeted metabolites were similar at both gestational stages, with less than 15% of the metabolites detected at only one stage (data not shown). AF, placenta, and maternal plasma shared 125 targeted metabolites, detected at both stages, but each matrix had some specific metabolites non-detected in other matrices (Figure 7A). Overall, 18% and 14% of the targeted metabolites in the placental and AF, respectively, were not detected in plasma. Although the metabolic composition of these 3 matrices was almost

similar, the concentrations of the different metabolites were quite different across the studied compartments, as shown in the score plot of the PCA (Figure 7B). PCA demonstrated that each matrix had a specific metabolome, the first principal component (PC1) showed the metabolic difference between placenta and the other two matrices accounting for 40% of the total variance (Figure 7B). Even if the specific metabolome of each matrix was dominant, the PCA also showed differences in metabolomes between GD13 and GD19, markedly in the placenta but less observable in the plasma.

Table 5: Statistical analysis (Wilcoxon rank-sum test, FDR corrected p value) between GD13 and GD19 stages for each matrix with total metabolites and matrix specific metabolites (n = 7).

GD13 vs GD19 stages	AF	Plasma	Placenta	Lipidomics Placenta
Discriminant metabolites $p(\text{FDR}) < 0.05$	88/186 (47%)	72/204 (35%)	136/173 (79%)	276/361 (76%)
Stable metabolites $p(\text{FDR}) > 0.5$	49/186 (26%)	38/204 (19%)	24/173 (15%)	28/361 (8%)

Additional statistical analyses were performed, on targeted data, to explore the differences between the two gestational stages in each matrix (Table 5). The main metabolic evolution was observed in the placenta. In the placenta, 79% and 76% of the metabolome and lipidome were significantly different (had different molecular intensities) between GD13 and GD19 ($p < 0.05$). In comparison, 47% of the AF metabolome and only 35% for the maternal plasma metabolome significantly differed between GD13 and GD19. These percentages also reflected the PCA (Figure 7B). The fact that almost half of the targeted metabolites differed between the two stages could be explained by the fact that both maternal and fetus metabolisms

occur in these mother-offspring interfaces making it very dynamic.⁴³ This is consistent with the results observed in women's placental metabolomics by Dunn and collaborators who described important changes in lipid metabolism during the early development of the placenta.⁴⁴ This important metabolic evolution of placenta metabolome is consistent with the wide array of structural and functional modifications of the placenta between these two stages.⁴⁵

The placenta and AF metabolomics also contained metabolites that displayed very little changes between the two gestational stages ($p>0.5$), revealing metabolic stability. In the AF and maternal plasma, 26% and 19% of the metabolites, respectively, did not change in intensity between the two stages ($p>0.5$). For the placental metabolome and lipidome, 15% and 8%, respectively, were stable. Interestingly, these stable metabolites were specific to each matrix (79% up to 82% were stable in only one matrix), none of the 125 metabolites was stable over time in the 3 matrices (Figure S6, Supporting Information).

Even with small samples collected from pregnant rodents, analyzing the metabolomics and lipidomics of the AF and placenta is an efficient tool to study prenatal metabolism evolution in pregnant rats and their fetuses. Even though each matrix had a highly specific metabolic profile, changes in the metabolomics profile over the gestation period were detectable.

4. CONCLUSIONS

As maternal–fetal metabolic communication involves also placenta, required for nutrient exchange; disorders of placenta could impact fetal development, while AF can be considered as an extension of the fetal extracellular space. Methods to extract the metabolome from

these matrices need to be validated in order to provide the maximum of information and robustness for biological studies. We evaluated the performance of different analytical methods for analysis of placenta and AF of rats to help each interested researchers to choose/optimize which method might be the best to move forward. The present work showed that MeOH and ACN extraction methods provided similar results and were suitable for studying AF metabolome. That said, MeOH provided slightly more efficient results for the AF metabolome in both C18- and HILIC-LC-MS platforms, in targeted and untargeted analyses. Despite the non-detection of some ionic metabolites using RP and HILIC chromatographic approaches, and the difficulty of identifying metabolites using untargeted approach, a good coverage of the metabolome was achieved using a multiplatform LC-MS analysis. NMR allowed to analyze/quantify in a reproducible way, without any extraction step, 41 metabolites in AF and was a complementary tool for 10% additional annotated metabolites to those analyzed by the combined C18- and HILIC-LC-MS (ESI+/ESI-). Lyophilization of the placental tissue did not impact the placental metabolome and lipidome, neither did the extraction solvent on the metabolome. However, MTBE provided more complete and reproducible extraction results on the lipidome in both targeted and untargeted analyses. LC-MS analyses of AF and placenta metabolomes allow rat gestational stages discrimination which could be a powerful tool to create a detailed metabolic profiling and identify biomarkers of fetal development and developmental diseases.

Supporting Information

Supporting Information contains **Figure S1**: Principal component analysis (PCA) score plot of targeted amniotic fluid metabolome using MeOH, ACN or MeOH/ACN extraction; **Table S1**:

List of polar metabolites (C18- and HILIC-LC-MS platforms ESI + /- modes); **Table S2**: NMR 1D and 2D assignments for rat AF from 150 μ L at 600 MHz compared to data from literature; **Figure S2**: Some AF quantified metabolites by ^1H NMR; **Figure S3**: Complementarity between C18- and HILIC-LC-MS, and NMR targeted annotation; **Figure S4**: Complementarity between wet or lyophilized tissue for each extraction solvent; **Table S3**: Reproducibility of metabolites detected in wet or lyophilized placenta; **Figure S5**: Principal component analysis score plot of placental lipidome with CH_2Cl_2 , MTBE and BuOH extraction solvent on wet or lyophilized tissue; **Figure S6**: Complementarity/specificity between matrices of stable metabolites between GD13 and GD19 stages; **Table S4**: Reproducibility of extracted metabolites and lipids in wet or lyophilized placental tissue in untargeted analyses.

Acknowledgements

This work was supported by the “Institut National de la Santé et de la Recherche” INSERM and the University of Tours. We thank the department “Analyse des Systèmes Biologiques” (PST ASB, Université de Tours, France) for their help with sample analyses. A. Bourdin-Pintueles received a grant from the French Ministry for National Education (bourse ministérielle - 2019-11).

REFERENCES

1. Zhang, A. H.; Sun, H.; Wang, P.; Han, Y.; Wang, X. J., Modern analytical techniques in metabolomics analysis. *Analyst* **2012**, *137* (2), 293-300.

2. De Paepe, E.; Van Meulebroek, L.; Rombouts, C.; Huysman, S.; Verplanken, K.; Lapauw, B.; Wauters, J.; Hemeryck, L. Y.; Vanhaecke, L., A validated multi-matrix platform for metabolomic fingerprinting of human urine, feces and plasma using ultra-high performance liquid-chromatography coupled to hybrid orbitrap high-resolution mass spectrometry. *Anal. Chim. Acta* **2018**, *1033*, 108-118.
3. Shen, L.; Liu, X.; Zhang, H.; Lin, J.; Feng, C.; Iqbal, J., Biomarkers in autism spectrum disorders: Current progress. *Clin. Chim. Acta* **2020**, *502*, 41-54.
4. Brown, A. G.; Tulina, N. M.; Barila, G. O.; Hester, M. S.; Elovitz, M. A., Exposure to intrauterine inflammation alters metabolomic profiles in the amniotic fluid, fetal and neonatal brain in the mouse. *PLoS One* **2017**, *12* (10), e0186656.
5. Bardanzellu, F.; Fanos, V., The choice of amniotic fluid in metabolomics for the monitoring of fetus health - update. *Expert Rev. Proteomics* **2019**, *16* (6), 487-499.
6. Wang, L.; Han, T. L.; Luo, X.; Li, S.; Young, T.; Chen, C.; Wen, L.; Xu, P.; Zheng, Y.; Saffery, R.; Baker, P. N.; Tong, C.; Qi, H., Metabolic Biomarkers of Monochorionic Twins Complicated With Selective Intrauterine Growth Restriction in Cord Plasma and Placental Tissue. *Sci. Rep.* **2018**, *8* (1), 15914.
7. Mussap, M.; Zaffanello, M.; Fanos, V., Metabolomics: a challenge for detecting and monitoring inborn errors of metabolism. *Ann. Transl. Med.* **2018**, *6* (17), 338.
8. Michaels, J. E.; Dasari, S.; Pereira, L.; Reddy, A. P.; Lapidus, J. A.; Lu, X.; Jacob, T.; Thomas, A.; Rodland, M.; Roberts, C. T., Jr.; Gravett, M. G.; Nagalla, S. R., Comprehensive proteomic analysis of the human amniotic fluid proteome: gestational age-dependent changes. *J. Proteome Res.* **2007**, *6* (4), 1277-85.
9. Menon, R.; Jones, J.; Gunst, P. R.; Kacerovsky, M.; Fortunato, S. J.; Saade, G. R.; Basraon, S., Amniotic fluid metabolomic analysis in spontaneous preterm birth. *Reprod. Sci.* **2014**, *21* (6), 791-803.
10. Vaughan, O. R.; Fowden, A. L., Placental metabolism: substrate requirements and the response to stress. *Reprod Domest Anim* **2016**, *51 Suppl 2*, 25-35.
11. Graça, G.; Duarte, I. F.; Goodfellow, B. J.; Barros, A. S.; Carreira, I. M.; Couceiro, A. B.; Spraul, M.; Gil, A. M., Potential of NMR Spectroscopy for the Study of Human Amniotic Fluid. *Anal. Chem.* **2007**, *79* (21), 8367-8375.
12. Virgiliou, C.; Gika, H. G.; Witting, M.; Bletsou, A. A.; Athanasiadis, A.; Zafrakas, M.; Thomaidis, N. S.; Raikos, N.; Makrydimas, G.; Theodoridis, G. A., Amniotic Fluid and Maternal Serum Metabolic Signatures in the Second Trimester Associated with Preterm Delivery. *J. Proteome Res.* **2017**, *16* (2), 898-910.
13. Orczyk-Pawilowicz, M.; Jawien, E.; Deja, S.; Hirnle, L.; Zabek, A.; Mlynarz, P., Metabolomics of Human Amniotic Fluid and Maternal Plasma during Normal Pregnancy. *PLoS One* **2016**, *11* (4), e0152740.
14. Gil, A. M.; Duarte, D., Biofluid Metabolomics in Preterm Birth Research. *Reprod. Sci.* **2018**, *25* (7), 967-977.
15. Walejko, J. M.; Chelliah, A.; Keller-Wood, M.; Gregg, A.; Edison, A. S., Global Metabolomics of the Placenta Reveals Distinct Metabolic Profiles between Maternal and Fetal Placental Tissues Following Delivery in Non-Labored Women. *Metabolites* **2018**, *8* (1), 10.
16. Fattuoni, C.; Mandò, C.; Palmas, F.; Anelli, G. M.; Novielli, C.; Parejo Laudicina, E.; Savasi, V. M.; Barberini, L.; Dessì, A.; Pintus, R.; Fanos, V.; Noto, A.; Cetin, I., Preliminary metabolomics analysis of placenta in maternal obesity. *Placenta* **2018**, *61*, 89-95.

17. Xie, H. H.; Xu, J. Y.; Xie, T.; Meng, X.; Lin, L. L.; He, L. L.; Wu, H.; Shan, J. J.; Wang, S. C., Effects of *Pinellia ternata* (Thunb.) Berit. on the metabolomic profiles of placenta and amniotic fluid in pregnant rats. *J. Ethnopharmacol.* **2016**, *183*, 38-45.
18. Rice, D.; Barone, S., Jr., Critical periods of vulnerability for the developing nervous system: evidence from humans and animal models. *Environ. Health Perspect.* **2000**, *108 Suppl 3 (Suppl 3)*, 511-33.
19. Cequier-Sanchez, E.; Rodriguez, C.; Ravelo, A. G.; Zarate, R., Dichloromethane as a solvent for lipid extraction and assessment of lipid classes and fatty acids from samples of different natures. *J. Agric. Food Chem.* **2008**, *56 (12)*, 4297-303.
20. Diémé, B.; Lefèvre, A.; Nadal-Desbarats, L.; Galineau, L.; Madji Hounoum, B.; Montigny, F.; Blasco, H.; Andres, C. R.; Emond, P.; Mavel, S., Workflow methodology for rat brain metabolome exploration using NMR, LC-MS and GC-MS analytical platforms. *J. Pharm. Biomed. Anal.* **2017**, *142*, 270-278.
21. Madji Hounoum, B.; Blasco, H.; Nadal-Desbarats, L.; Diémé, B.; Montigny, F.; Andres, C. R.; Emond, P.; Mavel, S., Analytical methodology for metabolomics study of adherent mammalian cells using NMR, GC-MS and LC-HRMS. *Anal. Bioanal. Chem.* **2015**, *407 (29)*, 8861-8872.
22. Dunn, W. B.; Broadhurst, D. I.; Atherton, H. J.; Goodacre, R.; Griffin, J. L., Systems level studies of mammalian metabolomes: the roles of mass spectrometry and nuclear magnetic resonance spectroscopy. *Chem. Soc. Rev.* **2011**, *40 (1)*, 387-426.
23. Broadhurst, D.; Goodacre, R.; Reinke, S. N.; Kuligowski, J.; Wilson, I. D.; Lewis, M. R.; Dunn, W. B., Guidelines and considerations for the use of system suitability and quality control samples in mass spectrometry assays applied in untargeted clinical metabolomic studies. *Metabolomics* **2018**, *14 (6)*, 72.
24. Pezzatti, J.; Boccard, J.; Codesido, S.; Gagnebin, Y.; Joshi, A.; Picard, D.; González-Ruiz, V.; Rudaz, S., Implementation of liquid chromatography-high resolution mass spectrometry methods for untargeted metabolomic analyses of biological samples: A tutorial. *Anal. Chim. Acta* **2020**, *1105*, 28-44.
25. Gerard, N.; Fahiminiya, S.; Grupen, C. G.; Nadal-Desbarats, L., Reproductive physiology and ovarian folliculogenesis examined via ¹H-NMR metabolomics signatures: a comparative study of large and small follicles in three mammalian species (*Bos taurus*, *Sus scrofa domestica* and *Equus ferus caballus*). *OMICS* **2015**, *19 (1)*, 31-40.
26. Le Guennec, A.; Dumez, J. N.; Giraudeau, P.; Caldarelli, S., Resolution-enhanced 2D NMR of complex mixtures by non-uniform sampling. *Magn. Reson. Chem.* **2015**, *53 (11)*, 913-920.
27. Guitton, Y.; Tremblay-Franco, M.; Le Corguillé, G.; Martin, J. F.; Pétéra, M.; Roger-Mele, P.; Delabrière, A.; Goulitquer, S.; Monsoor, M.; Duperier, C.; Canlet, C.; Servien, R.; Tardivel, P.; Caron, C.; Giacomoni, F.; Thévenot, E. A., Create, run, share, publish, and reference your LC-MS, FIA-MS, GC-MS, and NMR data analysis workflows with the Workflow4Metabolomics 3.0 Galaxy online infrastructure for metabolomics. *Int. J. Biochem. Cell. Biol.* **2017**, *93*, 89-101.
28. Nadal-Desbarats, L.; Veau, S.; Blasco, H.; Emond, P.; Royere, D.; Andres, C. R.; Guerif, F., Is NMR metabolic profiling of spent embryo culture media useful to assist in vitro human embryo selection? *MAGMA* **2013**, *26 (2)*, 193-202.
29. Bitar, T.; Mavel, S.; Emond, P.; Nadal-Desbarats, L.; Lefèvre, A.; Mattar, H.; Soufia, M.; Blasco, H.; Vourc'h, P.; Hleihel, W.; Andres, C. R., Identification of metabolic pathway

disturbances using multimodal metabolomics in autistic disorders in a Middle Eastern population. *J. Pharm. Biomed. Anal.* **2018**, *152*, 57-65.

30. Xia, J.; Bjorndahl, T. C.; Tang, P.; Wishart, D. S., MetaboMiner--semi-automated identification of metabolites from 2D NMR spectra of complex biofluids. *BMC Bioinformatics* **2008**, *9*, 507.

31. Chong, J.; Soufan, O.; Li, C.; Caraus, I.; Li, S.; Bourque, G.; Wishart, D. S.; Xia, J., MetaboAnalyst 4.0: towards more transparent and integrative metabolomics analysis. *Nucleic Acids Res.* **2018**, *46* (W1), W486-w494.

32. Mavel, S.; Nadal-Desbarats, L.; Blasco, H.; Bonnet-Brilhault, F.; Barthélémy, C.; Montigny, F.; Sarda, P.; Laumonnier, F.; Vourc'h, P.; Andres, C. R.; Emond, P., ¹H-¹³C NMR-based urine metabolic profiling in autism spectrum disorders. *Talanta* **2013**, *114*, 95-102.

33. Bardou, P.; Mariette, J.; Escudié, F.; Djemiel, C.; Klopp, C., jvenn: an interactive Venn diagram viewer. *BMC Bioinformatics* **2014**, *15* (1), 293.

34. Serriere, S.; Barantin, L.; Seguin, F.; Tranquart, F.; Nadal-Desbarats, L., Impact of prenatal stress on ¹H NMR-based metabolic profiling of rat amniotic fluid. *Magma* **2011**, *24* (5), 267-75.

35. Shan, J.; Xie, T.; Xu, J.; Zhou, H.; Zhao, X., Metabolomics of the amniotic fluid: Is it a feasible approach to evaluate the safety of Chinese medicine during pregnancy? *J. Appl. Toxicol.* **2019**, *39* (1), 163-171.

36. Carraro, S.; Baraldi, E.; Giordano, G.; Pirillo, P.; Stocchero, M.; Houben, M.; Bont, L., Metabolomic Profile of Amniotic Fluid and Wheezing in the First Year of Life-A Healthy Birth Cohort Study. *J. Pediatr.* **2018**, *196*, 264-269.e4.

37. Want, E. J.; Masson, P.; Michopoulos, F.; Wilson, I. D.; Theodoridis, G.; Plumb, R. S.; Shockcor, J.; Loftus, N.; Holmes, E.; Nicholson, J. K., Global metabolic profiling of animal and human tissues via UPLC-MS. *Nat. Protoc.* **2013**, *8* (1), 17-32.

38. Nagana Gowda, G. A.; Raftery, D., Can NMR solve some significant challenges in metabolomics? *Journal of Magnetic Resonance* **2015**, *260*, 144-160.

39. Chen, S.; Hoene, M.; Li, J.; Li, Y.; Zhao, X.; Häring, H. U.; Schleicher, E. D.; Weigert, C.; Xu, G.; Lehmann, R., Simultaneous extraction of metabolome and lipidome with methyl tert-butyl ether from a single small tissue sample for ultra-high performance liquid chromatography/mass spectrometry. *J. Chromatogr. A* **2013**, *1298*, 9-16.

40. Lofgren, L.; Stahlman, M.; Forsberg, G. B.; Saarinen, S.; Nilsson, R.; Hansson, G. I., The BUMER method: a novel automated chloroform-free 96-well total lipid extraction method for blood plasma. *J. Lipid Res.* **2012**, *53* (8), 1690-1700.

41. Pulkkinen, M. O.; Nyman, S.; Hämäläinen, M. M.; Mattinen, J., Proton NMR Spectroscopy of the Phospholipids in Human Uterine Smooth Muscle and Placenta. *Gynecol. Obstet. Invest.* **1998**, *46* (4), 220-224.

42. Troisi, J.; Symes, S.; Adair, D.; Colucci, A.; Prisco, S. E.; Aquino, C. I.; Vivone, I.; Guida, M.; Richards, S., Placental tissue metabolome analysis by GC-MS: Oven-drying is a viable sample preparation method. *Prep. Biochem. Biotech.* **2018**, *48* (6), 474-482.

43. Maltepe, E.; Fisher, S. J., Placenta: the forgotten organ. *Annu. Rev. Cell Dev. Biol.* **2015**, *31*, 523-52.

44. Dunn, W. B.; Brown, M.; Worton, S. A.; Davies, K.; Jones, R. L.; Kell, D. B.; Heazell, A. E. P., The metabolome of human placental tissue: investigation of first trimester tissue and changes related to preeclampsia in late pregnancy. *Metabolomics* **2012**, *8* (4), 579-597.

45. Furukawa, S.; Tsuji, N.; Sugiyama, A., Morphology and physiology of rat placenta for toxicological evaluation. *J. Toxicol. Pathol.* **2019**, *32* (1), 1-17.